Electrochemical Actuators Based on Two-Dimensional $Ti_3C_2T_x$ (MXene)

Di Pang[a], Mohamed Alhabeb[b], Xinpeng Mu[a], Yohan Dall'Agnese[c], Yury Gogotsi[a,b]*, Yu Gao[a]**

[a]Key Laboratory of Physics and Technology for Advanced Batteries (Ministry of Education), College of Physics, Jilin University, Changchun 130012, PR China

[b]A.J. Drexel Nanomaterials Institute, Department of Materials Science and Engineering, Drexel University, Philadelphia, PA 19104, United States

[c]Institute for Materials Discovery, University College London, London WC1E 7JE, United Kingdom

Abstract: Electrochemical actuators are devices that convert electrical energy into mechanical energy via electrochemical processes. They are used in soft robotics, artificial muscles, micro-pumps, sensors and other fields. The design of flexible and stable electrode materials remains a major challenge. MXenes, an emerging family of 2D materials, have found applications in energy storage. Here, we report an actuator device using MXene ($Ti_3C_2T_x$) as a flexible electrode material. The electrode in 1 M H_2SO_4 electrolyte exhibits a curvature's change up to 0.083 mm^{-1} and strain of 0.29%. Meanwhile, the MXene-based actuator with a symmetric configuration separated by gel electrolyte (PVA-H_2SO_4) has curvature and strain changes up to 0.038 mm^{-1} and 0.26% with excellent retention after 10,000 cycles. In-situ X-ray diffraction analysis demonstrates that the actuation mechanism is due to the expansion and shrinkage of the interlayer spacing of MXenes. This research shows promise of this new family of materials for electrochemical actuators.

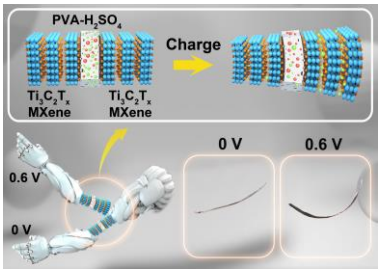

Keywords: 2D materials, MXene, electrochemical actuators, *in-situ* X-ray diffraction, soft robotics

Actuators are devices that convert electrical energy into mechanical energy under external stimuli (e.g., heat, light, temperature, pH, electrochemical, etc.).[1-2] Their applications include artificial muscles, converters, soft robotics, nano- and micro-electromechanical systems, bionics, and switches.[3-5] Ionic electroactive polymers have received extensive attention in the field of actuation devices due to their advantages such as large displacement and deformation under low voltage (<5 V).[6-8] Ionic electroactive polymer actuation materials include polymer gels, conductive polymers and ionic polymer metal composites (IPMC).[9-10] When using polymer gel and conductive polymer, it is difficult to realize the transition from material to device because of the limited ion diffusion rate leading to slow actuation. IPMC electrochemical actuators, have become a research focus due to light weight, fast response rate and large displacement under low voltage.[11-12] In 1999, Baughman *et al*. reported the first carbon nanotube (CNTs) actuators driven by quantum stretching effects in aqueous electrolytes.[1] Since then, CNTs have been extensively studied because of their large specific surface area, light weight, high conductivity and good mechanical properties, and have been proposed for artificial muscles, MEMS, and other applications.[3, 13-15] In recent years, numerous other materials have been investigated as electrodes for actuators, including graphene,[16] graphdiyne[17] and 2D MoS_2,[18] but achieving a combination of properties required for fast actuation at low working voltage (1 V), such as high electronic and ionic conductivity, high stability, and mechanical strength combined with flexibility remains a major challenge.

In 2011, a large family of two-dimensional transition metal carbides and nitrides called MXenes was discovered at Drexel University.[19-20] MXenes, in particular $Ti_3C_2T_x$, exhibit fast charge storage ability, excellent electronic/ionic conductivity and high mechanical strength.[21-22] $Ti_3C_2T_x$ is under extensive investigation in various research areas, including energy storage and conversion.[23-28] $Ti_3C_2T_x$ exhibited excellent performance as an electrode for supercapacitors at

extremely high rates, with the ability to be charged in milliseconds in sulfuric acid (H_2SO_4).[29] Recently, *in-situ* X-ray diffraction (XRD) demonstrated an expansion and shrinkage of the lattice of $Ti_3C_2T_x$ during cycling in H_2SO_4, which should lead to the actuation phenomenon.[30] The actuation of $Ti_3C_2T_x$ upon Na^+, Li^+, K^+ and Mg^{2+} intercalation was studied by atomic force microscopy in the direction normal to the electrode plane.[31] A bilayer-structured actuator based on MXene ($Ti_3C_2T_x$)-cellulose composites and polycarbonate membrane has been reported.[32] Recently, poly(3,4 ethylenedioxythiophene)-poly(styrenesulfonate) with up to 40% $Ti_3C_2T_x$ electrode showed promising performance for kinetic soft robotics,[33] yet pristine $Ti_3C_2T_x$ as electrode for electrochemical actuators remains unexplored.

In this work, we report that two-dimensional $Ti_3C_2T_x$ MXene can be used as a flexible electrode material for electrochemical actuators. This paper focuses on the preparation, assembly, and actuation performance of $Ti_3C_2T_x$ with liquid 1 M H_2SO_4 and polyvinyl alcohol sulfuric acid gel (PVA-H_2SO_4) electrolytes. H_2SO_4 was selected because it showed the largest capacity and substantive expansion and shrinkage phenomenon in aqueous electrolytes.[15,34] PVA was used as the polymer matrix and mixed with sulfuric acid for solid-state actuators because PVA has a good solubility in water, low cost, good electrochemical stability, and PVA-MXene films can be made thin and flexible. The Young's modulus values of $Ti_3C_2T_x$ film and PVA-$Ti_3C_2T_x$ composite were reported to be 3.52 GPa and 3.7 GPa, respectively.[34] Encouraging actuation performance were achieved, with curvature and linear strain up to 0.083 mm^{-1} of 0.29% in 1 M H_2SO_4. *In-situ* XRD study confirms that the actuation mechanism of MXenes ($Ti_3C_2T_x$) is interlayer expansion and shrinkage due to protons intercalation, de-intercalation and redox reaction during charge and discharge. Additionally, water molecules are spontaneously intercalated between layers,[35] but there is no indication that the H_2O content changes with charging/discharging MXenes.

The actuation of a single $Ti_3C_2T_x$ MXene electrode in 1 M H_2SO_4 was investigated by preparing a conductive and electrochemically active freestanding $Ti_3C_2T_x$ MXene strip (15 µm thick, 4 cm long, 5 mm wide). Figure 1a is a scanning electron microscopy (SEM) image of $Ti_3C_2T_x$, which shows the aligned layered morphology of the electrode. A 40 µm commercial Scotch tape was used to cover one side of the MXene strip. Then the electrode was immersed in 1 M H_2SO_4 and connected to a potentiostat in a 3-electrode configuration, as shown in Figure 1b. Cyclic voltammetry from -0.8 V to +0.2 V vs. Ag wire at different rates was used to induce the actuation.

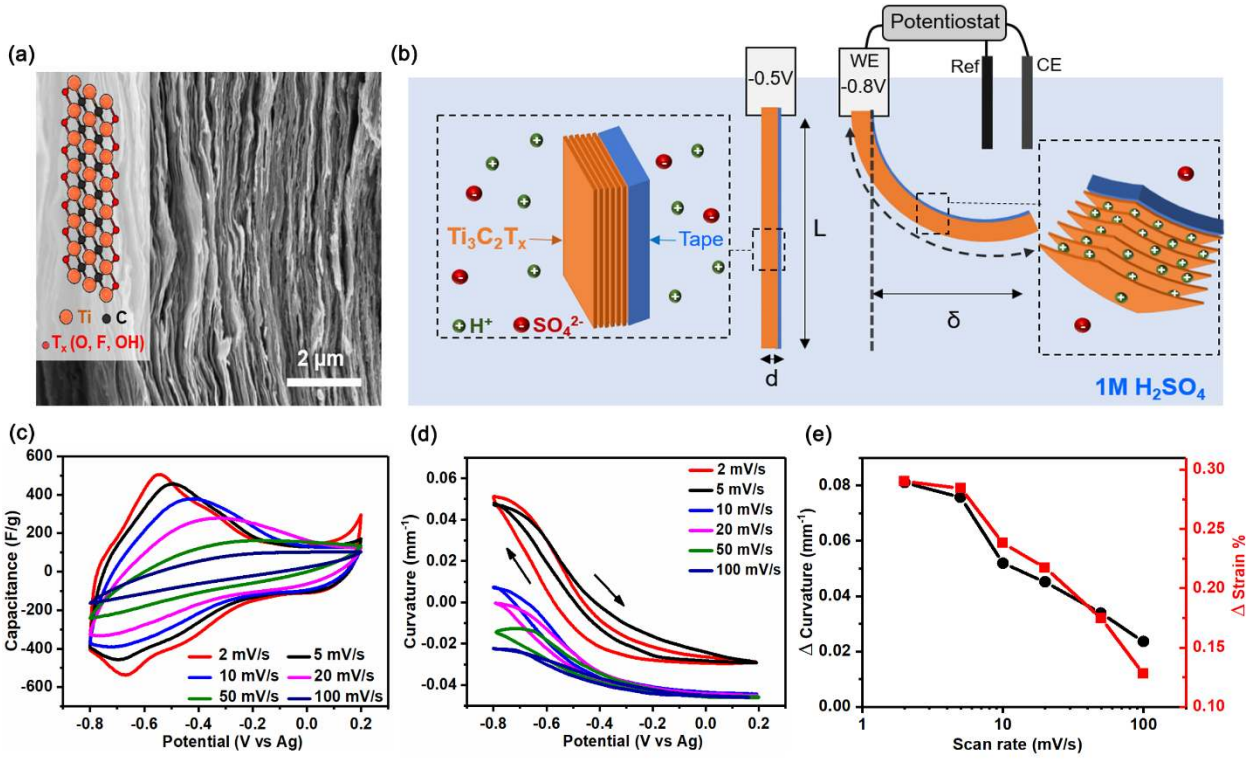

Figure 1. (a) Cross-sectional scanning electron microscopy image of a $Ti_3C_2T_x$ electrode. (b) Schematic representation of the actuator setup in 1 M H_2SO_4 (the curvature corresponds to 2 mV/s rate). (c) Cyclic voltammograms, (d) curvature as a function of applied potential, and (e) difference in curvature and strain at different scan rates.

Figure 1c and S1a show the cyclic voltammograms and corresponding capacitances obtained at different scan rates. The cyclic voltammograms are similar to previous reports,[36] with the presence of broad redox peaks below -0.2 V *vs*. Ag. The curves appear to be more resistive than previously reported, especially at higher scan rates, which might come from the relatively thicker and longer electrode and the lack of current collectors. A consequence of the higher resistance is that the capacitances measured, from 247 F/g at 2 mV/s to 72 F/g at 100 mV/s, are lower than the state-of-the-art $Ti_3C_2T_x$-based supercapacitor.[37] However, high conductivity of the film (~4,000 S/cm) allowed the use of current collector-free electrodes. Thus, no energy is wasted on bending a passive metal foil.

The displacement during cyclic voltammetry was measured and the actuation performance, expressed in curvature and strain, was calculated (see Methods). Supplementary Video S1 and Figure S2 are records of the electrode deformation during cyclic voltammetry at 2 mV/s. Figure 1d shows the curvature obtained from -0.8 V to +0.2 V *vs*. Ag wire at different rates. The curvature change is not linear with the potential and there is a small hysteresis between the charge and discharge. The downward curvature shift between different scan rates is due to the change of the scan rate, from 2 to 100 mV/s. In the -0.3 V to +0.2 V *vs*. Ag range, there is an almost negligible curvature change. In contrast, a large actuation phenomenon occurs in the range from -0.8 V to -0.3 V *vs*. Ag, with a curvature change up to 0.08 mm^{-1}. This is in agreement with the shape of the cyclic voltammograms and previous *in-situ* XRD results,[30] because the actuation phenomenon is due to protons intercalation between $Ti_3C_2T_x$ layers and =O to -OH change in the surface termination below -0.3 V *vs*. Ag, which is accompanied by lattice expansion.

Figure 1e shows the strain and difference in curvature calculated at each scan rate. The actuation decreases with increasing scan rate, proportionally to the capacitance decrease. The maximum

strain and difference in curvature at 2 mV/s are 0.289% and 0.081 mm^{-1}, respectively, which is superior to most of graphene-based actuators.[16] Figure S1b shows a quasi linear relationship between capacitance and curvature, confirming that the actuation performance is closely related to the electrochemical performance of $Ti_3C_2T_x$. At 100 mV/s (20 seconds charge/discharge), curvature of 0.0236 mm^{-1} and strain of 0.128% were measured. This actuator was also tested under frequencies from 1 mHz to 1 Hz, as shown Figure S3a. As expected, the actuation performance decreases with increasing frequency. At a frequency of 1 mHz, the curvature and strain reach up to 0.083 mm^{-1} and 0.29%, but at 1 Hz, the performance decreases to 0.0043 mm^{-1} and 0.025%.

The actuation of $Ti_3C_2T_x$ in 1 M H_2SO_4 is promising, however it is unlikely that real actuator applications can be performed in liquid sulfuric acid electrolyte. Indeed, actuators, such as robotic arms, illustrated in Figure 2a, must work in air. Therefore, a prototype of a solid-state MXene-based actuator was developed using symmetric $Ti_3C_2T_x$ strip electrodes separated by PVA-H_2SO_4 solid electrolyte, as illustrated in Figure 2b-c. Figure S4 shows a cross-sectional SEM image of the solid actuator where the sandwich configuration is identifiable. It can be seen that the solid electrolyte has a good adhesion to $Ti_3C_2T_x$ electrodes.

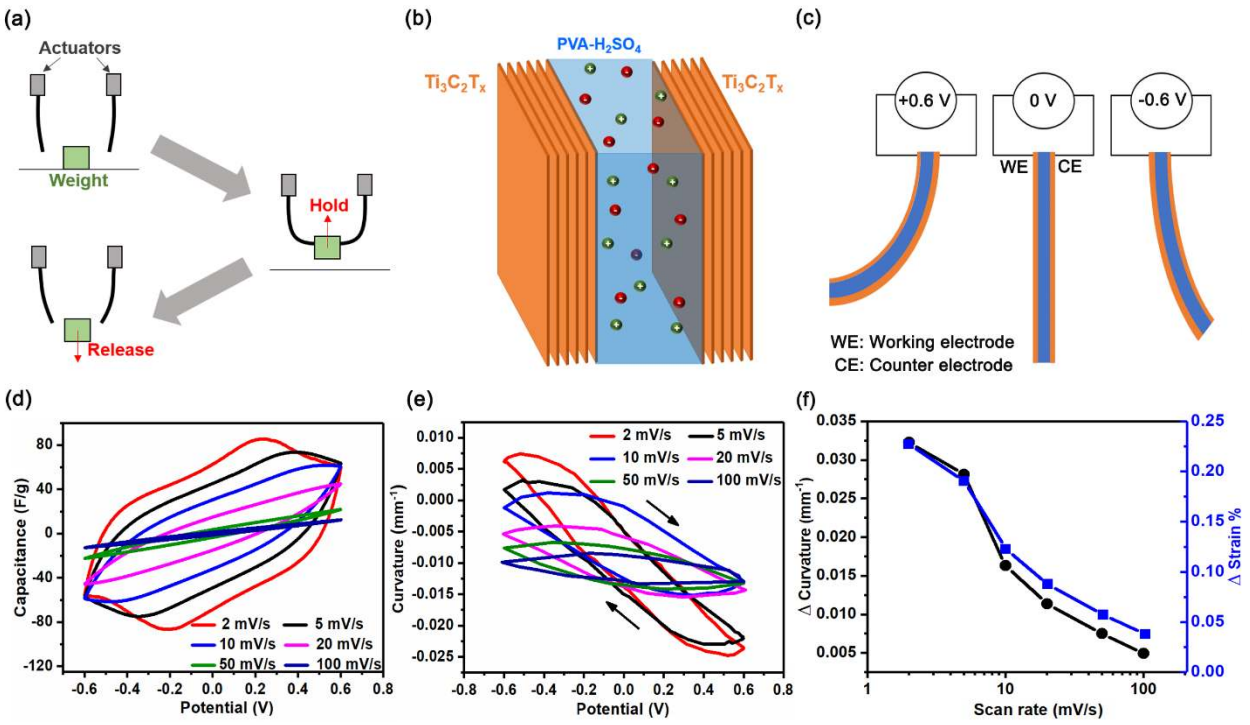

Figure 2. Schematic illustrations of (a) MXene robotic arms, (b) the $Ti_3C_2T_x$/PVA-H_2SO_4/$Ti_3C_2T_x$ actuator configuration, and (c) motion during cycling at 2 mV/s. (d) Cyclic voltammograms, (e) curvature, and (f) difference in curvature and strain at different scan rates.

Figure 2d shows the cyclic voltammograms obtained in a -0.6 V to +0.6 V potential range at different scan rates. The curves are symmetric, as expected from a symmetric configuration. However, the curves become more resistive with increasing scan rate to the point that there is almost no capacitance above 50 mV/s. This is attributed to the ionic resistance of solid electrolyte. Figure S1a shows a summary of the capacitance at the different scan rates. Note that the gravimetric capacitance was calculated per weight of both electrodes. The highest capacitance was 55 F/g, although it is fair to mention that contrary to supercapacitor application the actuator device was cycled in both positive and negative range to maximize the displacement. It is unsurprising that the electrochemical performance is lower than in liquid H_2SO_4 because PVA-H_2SO_4 has a

lower conductivity. Specifically, the ionic conductivity of the gel polymer electrolyte is about 10^{-3} S/cm, whereas 1 M H_2SO_4 conductivity is 0.8 S/cm. It means that the migration, diffusion and intercalation of protons in solid electrolyte is slower and overall fewer protons can be inserted due to time limitation.

Figure 2e shows the curvature response during cyclic voltammetry. Video S2 and Figure S5 show the corresponding actuator motion. Because the charge storage and proton intercalation are limited by the conductivity of the electrolyte, it is logical that the corresponding curvature is affected. Indeed, significantly smaller actuations is observed compared to 1 M H_2SO_4, partially due to the lower conductivity and capacitance, but also because the PVA-H_2SO_4 solid electrolyte layer and the second electrode decrease the overall flexibility of the actuator. The curvature response with potential is symmetric, in contrast to results obtained in 1 M H_2SO_4, due to the symmetric configuration used. Figure 2f shows difference in curvature and strain at each scan rate tested, and Figure S1c confirm the quasi-linear dependence between the capacitance and curvature. The highest curvature and strain obtained are 0.0323 mm^{-1} and 0.227%, which is respectively 40% and 78% of the performance in 1 M H_2SO_4, thus exceeding many previously proposed actuators (Table S1). Important to note that this performance was achieved at low voltage and using inexpensive electrolyte that is not air sensitive and does not require special sealing, unlike organic electrolytes.

Additionally, this device was tested at various frequencies, shown in Figure S3d. The curvature and strain are 0.038 mm^{-1} and 0.26% at 1 mHz. However, the performance decreases with increasing frequency, until reaching zero at 0.5 Hz.

Previous work investigating the actuation phenomenon of $Ti_3C_2T_x$ upon electrochemical intercalation/de-intercalation of Li^+, Na^+, K^+ or Mg^{2+} by atomic force microscopy[31] and recently

in-situ XRD of $Ti_3C_2T_x$ in 1 M H_2SO_4 demonstrated the volume change upon H^+ insertion,[30] which correlates well with the actuation observed. To further demonstrate the actuation mechanism, *in-situ* XRD analysis of the $Ti_3C_2T_x$/PVA-H_2SO_4/$Ti_3C_2T_x$ based actuator was performed. Figure S6 shows the XRD patterns and *c*-lattice parameter changes of $Ti_3C_2T_x$ during cyclic voltammetry. Overall, during cycling, the interlayer spacing shrinks/expandes by up to 0.11 Å. These results are in agreement with previous studies in liquid electrolyte,[30] but the lattice change is smaller which may be due to the lower capacitance and contrain of PVA gel. This small expansion/shrinkage of the lattice results in a larger macroscopic expansion and shrinkage of the electrode, which is responsible for the actuation phenomenon.

Another important parameter for practical application of an actuator is its cycle life. The actuator was subjected to 10,000 cycles through galvanostatic charge/discharge at 500 mA g^{-1}, as seen in Figure 3. At first, the actuation performance increased with the cycle number, to reach a maximum after 1000 cycles. This self-improving phenomenon might be due to improved permeation of protons between MXene layers. Then, the curvature starts to decrease, which might be due to the either mechanical or chemical aging of electrodes. 80.4% of the initial performance remained after 10,000 cycles.

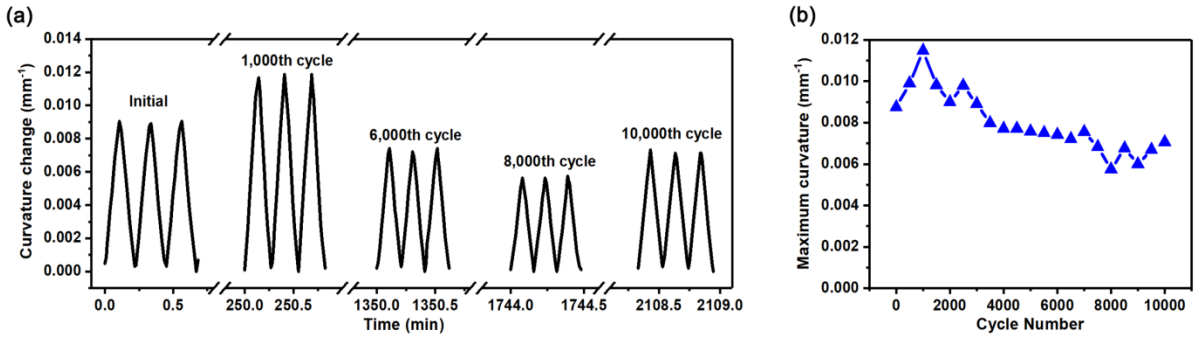

Figure 3. (a) Bending curvature change under galvanostatic charge-discharge at 500 mA g^{-1}. (b) Cycling performance of the PVA-H_2SO_4/$Ti_3C_2T_x$ actuator.

This MXene-based actuator can be used for application in soft robotics, for example performing the task illustrated in Figure 2a, as demonstrated in Video S3 (supplementary information). The weight carried in this experiment is 2.8 times heavier than the weight of the actuators, demonstrating the potential of this device. Video S4 is another example of application in which a single actuator carried an object 5.3 times its own weight. Many other applications can be envisioned, such as electrical on/off switching, tuneable lenses and other optical devices, since transparent and electrochromic MXene supercapacitors have been demonstrated.[38] Taking into account that $Ti_3C_2T_x$ has higher mechanical properties and electronic conductivity than solution-processed graphene, further performance improvement is certainly expected. Since more about 30 different MXenes are available and many more are under development,[19] all having different colors and different mechanical and electronic properties, there is plenty of room for exploration of MXenes use in electrochemical actuation. And, of course, those MXenes can be matched with different electrolytes to control the expansion of the interlayer spacing and their actuation.

Use of $Ti_3C_2T_x$ MXene as electrochemical actuator has been demonstrated in two device configurations. In 1 M H_2SO_4 electrolyte, a single $Ti_3C_2T_x$ electrode operating at 1 V can reach curvature up to 0.083 mm^{-1} and strain value of 0.29%, which is close to graphene.[16] In the second design, using two symmetric $Ti_3C_2T_x$ electrodes separated by PVA-H_2SO_4 solid electrolyte, the curvature and strain reach up to 0.038 mm^{-1} and 0.26%, which is somewhat lower due to the thicker device and lower conductivity of solid electrolyte, but promising for practical applications. The actuation retention was excellent, with a slight increase during the first 1000 cycles and still 80.4% of the initial curvature after 10,000 cycles. The actuation was attributed to the interlayer space change of $Ti_3C_2T_x$ upon intercalation/de-intercalation of protons between $Ti_3C_2T_x$ layers, which was confirmed by *in-situ* XRD.

These results open a new field of applications for MXenes and demonstrate the potential of MXenes in this field. Yet the performance could be further improved by optimizing the actuator design, using a thinner solid electrolyte, an organic electrolyte with a wider voltage window, or a different MXene composition.

ASSOCIATED CONTENT

Supporting Information.

Experiment methods, capacitances test result, capacitance vs. curvature curves, the experimental images, SEM image, frequency to actuation performance test results, *in-situ* X-ray diffraction data, a table of actuation performance comparison, and Video (S1-S4).

AUTHOR INFORMATION

Corresponding Author

y.dallagnese@ucl.ac.uk (Y. Dall'Agnese)

gogotsi@drexel.edu (Y. Gogotsi)

yugao@jlu.edu.cn (Y. Gao)

Notes

The authors declare no competing financial interest.

ACKNOWLEDGMENT

This work was supported by the Science & Technology Department of Jilin Province (No. 20180101199JC, 20180101204JC) and Jilin Province/Jilin University Co-construction Project-Funds for New Materials (SXGJSF2017-3).

REFERENCES

(1) Baughman, R. H.; Cui, C.; Zakhidov, A. A.; Iqbal, Z.; Barisci, J. N.; Spinks, G. M.; Wallace, G. G.; Mazzoldi, A.; De Rossi, D.; Rinzler, A. G.; Jaschinski, O.; Roth, S.; Kertesz, M. Carbon Nanotube Actuators. *Science* **1999,** *284* (5418), 1340-1344.

(2) Ma, M.; Guo, L.; Anderson, D. G.; Langer, R. Bio-Inspired Polymer Composite Actuator and Generator Driven by Water Gradients. *Science* **2013,** *339* (6116), 186-189.

(3) Aliev, A. E.; Jiyoung, O.; Kozlov, M. E.; Kuznetsov, A. A.; Shaoli, F.; Fonseca, A. F.; Raquel, O.; Lima, M. D.; Haque, M. H.; Gartstein, Y. N. Giant-stroke, superelastic carbon nanotube aerogel muscles. *Science* **2009,** *323* (5921), 1575-1578.

(4) Brochu, P.; Pei, Q. Advances in Dielectric Elastomers for Actuators and Artificial Muscles. *Macromol. Rapid Commun.* **2010,** *31* (1), 10-36.

(5) Zhao, Y.; Song, L.; Zhang, Z.; Qu, L. Stimulus-responsive graphene systems towards actuator applications. *Energy Environ. Sci.* **2013,** *6* (12), 3520-3536.

(6) Ohalloran, A.; Omalley, F.; Mchugh, P. A review on dielectric elastomer actuators, technology, applications, and challenges. *J. Appl. Phys.* **2008,** *104* (7), 9.

(7) Barcohen, Y., *Electroactive Polymer (EAP) Actuators as Artificial Muscles: Reality, Potential, and Challenges*. SPIE: Bellingham, WA, **2004**.

(8) Sewa, S.; Onishi, K.; Asaka, K.; Fujiwara, N.; Oguro, K. In *Polymer actuator driven by ion current at low voltage, applied to catheter system*, Proc. MEMS 98, IEEE: **1998**; pp 148-153.

(9) Shahinpoor, M.; Bar-Cohen, Y.; Simpson, J. O.; Smith, J. Ionic polymer-metal composites (IPMCs) as biomimetic sensors, actuators and artificial muscles - a review. *Smart Mater. Struct.* **1998,** *7* (6), 251-267.

(10) Shahinpoor. Continuum electromechanics of ionic polymeric gels as artificial muscles for robotic applications. *Smart Mater. Struct.* **1994,** *3* (3), 367.

(11) Wu, G.; Hu, Y.; Zhao, J.; Lan, T.; Wang, D.; Liu, Y.; Chen, W. Ordered and Active Nanochannel Electrode Design for High-Performance Electrochemical Actuator. *Small* **2016,** *12* (36), 4986-4992.

(12) Li, J.; Ma, W.; Song, L.; Niu, Z.; Cai, L.; Zeng, Q.; Zhang, X.; Dong, H.; Zhao, D.; Zhou, W. Superfast-Response and Ultrahigh-Power-Density Electromechanical Actuators Based on Hierarchal Carbon Nanotube Electrodes and Chitosan. *Nano Lett.* **2011,** *11* (11), 4636.

(13) Fukushima, T.; Asaka, K.; Kosaka, A.; Aida, T. Fully Plastic Actuator through Layer-by-Layer Casting with Ionic-Liquid-Based Bucky Gel. *Angew. Chem. Int. Ed.* **2010,** *44* (16), 2410-2413.

(14) Terasawa, N.; Mukai, K.; Yamato, K.; Asaka, K. Superior performance of non-activated multi-walled carbon nanotube polymer actuator containing ruthenium oxide over a single-walled carbon nanotube. *Carbon* **2012,** *50* (5), 1888-1896.

(15) Benoit, J. M.; Gu, G.; Kim, G. T.; Minett, A.; Baughman, R.; Roth, S. Actuators of individual carbon nanotubes. *Curr. Appl Phys.* **2002,** *2* (4), 311-314.

(16) Xie, X.; Qu, L.; Zhou, C.; Li, Y.; Zhu, J.; Bai, H.; Shi, G.; Dai, L. An Asymmetrically Surface-Modified Graphene Film Electrochemical Actuator. *ACS Nano* **2010,** *4* (10), 6050-4.

(17) Chao, L.; Ying, Y.; Jian, W.; Fu, R.; Chen, W. High-performance graphdiyne-based electrochemical actuators. *Nat. Commun.* **2018,** *9* (1), 752.

(18) Acerce, M.; Akdoğan, E. K.; Chhowalla, M. Metallic molybdenum disulfide nanosheet-based electrochemical actuators. *Nature* **2017,** *549*, 370.

(19) Anasori, B.; Gogotsi, Y., *2D Metal Carbides and Nitrides (MXenes)*. Springer International **2019**; p VIII, 570.

(20) Naguib, M.; Kurtoglu, M.; Presser, V.; Lu, J.; Niu, J.; Heon, M.; Hultman, L.; Gogotsi, Y.; Barsoum, M. W. Two-dimensional nanocrystals produced by exfoliation of Ti_3AlC_2. *Adv. Mater.* **2011,** *23* (37), 4248-4253.

(21) Hart, J. L.; Hantanasirisakul, K.; Lang, A. C.; Anasori, B.; Pinto, D.; Pivak, Y.; van Omme, J. T.; May, S. J.; Gogotsi, Y.; Taheri, M. L. Control of MXenes' electronic properties through termination and intercalation. *Nat. Commun.* **2019,** *10* (1), 522.

(22) Lipatov, A.; Lu, H.; Alhabeb, M.; Anasori, B.; Sinitskii, A. Elastic properties of 2D $Ti_3C_2T_x$ MXene monolayers and bilayers. *Sci. Adv.* **2018,** *4* (6), eaat0491.

(23) VahidMohammadi, A.; Hadjikhani, A.; Shahbazmohamadi, S.; Beidaghi, M. Two-Dimensional Vanadium Carbide (MXene) as a High-Capacity Cathode Material for Rechargeable Aluminum Batteries. *ACS Nano* **2017,** *11* (11), 11135-11144.

(24) Yang, L.; Dall'Agnese, Y.; Hantanasirisakul, K.; Shuck, C. E.; Maleski, K.; Alhabeb, M.; Chen, G.; Gao, Y.; Sanehira, Y.; Jena, A. K.; Shen, L.; Dall'Agnese, C.; Wang, X. F.; Gogotsi, Y.; Miyasaka, T. SnO_2-Ti_3C_2 MXene electron transport layers for perovskite solar cells. *J. Mater. Chem. A* **2019,** *7* (10), 5635-5642.

(25) Ran, J.; Gao, G.; Li, F.-T.; Ma, T.-Y.; Du, A.; Qiao, S.-Z. Ti_3C_2 MXene co-catalyst on metal sulfide photo-absorbers for enhanced visible-light photocatalytic hydrogen production. *Nat. Commun.* **2017,** *8*, 13907.

(26) Beidaghi, M.; Gogotsi, Y. Capacitive energy storage in micro-scale devices: recent

advances in design and fabrication of micro-supercapacitors. *Energy Environ. Sci.* **2014,** *7* (3), 867-884.

(27) Sun, Y.; Sun, Y.; Meng, X.; Gao, Y.; Dall'Agnese, Y.; Chen, G.; Dall'Agnese, C.; Wang, X.-F. Eosin Y-sensitized partially oxidized Ti_3C_2 MXene for photocatalytic hydrogen evolution. *Catal. Sci Technol.* **2019,** *9(2)*, 310-315.

(28) Anasori, B.; Lukatskaya, M. R.; Gogotsi, Y. 2D metal carbides and nitrides (MXenes) for energy storage. *Nat. Rev. Mater.* **2017,** *2* (2), 16098.

(29) Gund, G. S.; Park, J. H.; Harpalsinh, R.; Kota, M.; Shin, J. H.; Kim, T.-i.; Gogotsi, Y.; Park, H. S. MXene/Polymer Hybrid Materials for Flexible AC-Filtering Electrochemical Capacitors. *Joule* **2019,** *3* (1), 164-176.

(30) Mu, X.; Wang, D.; Du, F.; Chen, G.; Wang, C.; Wei, Y.; Gogotsi, Y.; Gao, Y.; Dall'Agnese, Y. Revealing the Pseudo-Intercalation Charge Storage Mechanism of MXenes in Acidic Electrolyte. *Adv. Funct. Mater.* **2019,** *0* (0), 1902953.

(31) Come, J.; Black, J. M.; Lukatskaya, M. R.; Naguib, M.; Beidaghi, M.; Rondinone, A. J.; Kalinin, S. V.; Wesolowski, D. J.; Gogotsi, Y.; Balke, N. Controlling the actuation properties of MXene paper electrodes upon cation intercalation. *Nano Energy* **2015,** *17*, 27-35.

(32) Cai, G.; Ciou, J.-H.; Liu, Y.; Jiang, Y.; Lee, P. S. Leaf-inspired multiresponsive MXene-based actuator for programmable smart devices. *Sci. Adv.* **2019,** *5* (7), eaaw7956.

(33) Umrao, S.; Tabassian, R.; Kim, J.; Nguyen, V. H.; Zhou, Q.; Nam, S.; Oh, I.-K. MXene artificial muscles based on ionically cross-linked $Ti_3C_2T_x$ electrode for kinetic soft robotics. *Science Robotics* **2019,** *4* (33), eaaw7797.

(34) Ling, Z.; Ren, C. E.; Zhao, M.-Q.; Yang, J.; Giammarco, J. M.; Qiu, J.; Barsoum, M. W.; Gogotsi, Y. Flexible and conductive MXene films and nanocomposites with high capacitance. *Proc.*

Natl. Acad. Sci. U. S. A. **2014,** *111* (47), 16676-81.

(35) Ghidiu, M.; Halim, J.; Kota, S.; Bish, D.; Gogotsi, Y.; Barsoum, M. Ion-Exchange and Cation Solvation Reactions in Ti_3C_2 MXene. *Chem. Mater.* **2016,** *28*.

(36) Xia, Y.; Mathis, T. S.; Zhao, M.-Q.; Anasori, B.; Dang, A.; Zhou, Z.; Cho, H.; Gogotsi, Y.; Yang, S. Thickness-independent capacitance of vertically aligned liquid-crystalline MXenes. *Nature* **2018,** *557* (7705), 409-412.

(37) Lukatskaya, M. R.; Kota, S.; Lin, Z.; Zhao, M.-Q.; Shpigel, N.; Levi, M. D.; Halim, J.; Taberna, P.-L.; Barsoum, M. W.; Simon, P. Ultra-high-rate pseudocapacitive energy storage in two-dimensional transition metal carbides. *Nat. Energy* **2017,** *2*, 17105.

(38) Salles, P.; Pinto, D.; Hantanasirisakul, K.; Maleski, K.; Shuck, C. E.; Gogotsi, Y. Electrochromic Effect in Titanium Carbide MXene Thin Films Produced by Dip-Coating. *Adv. Funct. Mater.* **2019,** *29* (17), 1809223.